Electronic Supplementary Information for

Bimodal porous superparticles with the optimized structure prepared by self-limited aggregation of PEG-coated mesoporous nanofibers for purification of protein-dye conjugates

Kaka Zhang, Junqi Yi, and Daoyong Chen*

The State Key Laboratory of Molecular Engineering of Polymers and Department of Macromolecular Science
Fudan University, Handan Road 220, Shanghai 200433, P. R. China.
* E-mail: chendy@fudan.edu.cn

Table of Contents

S1. Deposition of $mSiO_2$ onto the quaternized P4VP cores

In our system, the $mSiO_2$ deposited onto the quaternized P4VP cores. It is noteworthy that although the PEG shells consisting of PEG chains with high grafting density can resist the adsorption of proteins, they can still allow diffusion of small molecules and small nanoparticles sized below 2 nm into the quaternized P4VP cores, which is necessary for the deposition of the as-formed small $mSiO_2$ nanoparticles.

S2. Calculation of the thickness of PEG-5000 polymer brushes of the nanofibers

According to de Gennes's theoretical study (ref 31 in the main text), the thickness L of the polymer brushes can be calculated by the equation $L=Na\sigma^{1/3}$, where N is the degree of polymerization, a the mesh size in the Flory-Huggins lattice model, and σ the grafting fraction. Na equals to the contour length of the polymer chains, and for PEG-5000 it is 42 nm. The grafting fraction σ equal to a^2/D^2, where D is the average distance between grafted sites on the surface. For our nanofibers, the number of grafted chains per square nanometers $1/D^2$ can be calculated from the molecular weight of the polymeric nanofibers by static light scattering (ref 24 in the main text) to be 0.32. And the area of EG monomer on the surface a^2 can be estimated from the density of PEG-5000 (1.094 g/mL) and the molecular weight of EG (44 g/mol) to be 0.165 nm^2. Thus the thickness of the PEG-5000 polymer brushes of the nanofibers was estimated to be 16 nm.

S3. Two factors further support the conclusion that the thickness of PEG shell is larger than that of the $mSiO_2$ layer surronding the quaternized P4VP core

First, in the hybrid nanofibers, there are $mSiO_2$ embedded within the quaternized P4VP core, and thus the diameter of the core is larger than 21 nm. So the thickness of $mSiO_2$ layer surrounding the quaternized P4VP core is less than 7.5 nm. Second, the $mSiO_2$ layer surrounding the core surface makes the PEG chains more crowded and thus more stretched. This should further increase the thickness of the PEG shell, i.e., the actual thickness of the PEG shell is larger than 16 nm.

S4. The explanation of the step in the nitrogen sorption isotherm

As described in the main text, in the isotherm of the superparticles, a step at relative pressure of 0.26 corresponding to the mesopores of 2 nm in pore size was detected; TEM also confirmed that the pore size of $mSiO_2$ in the superparticles is approximately 2 nm. In the control experiment, we prepared $mSiO_2$ (denoted as control $mSiO_2$) under the same conditions as those for preparing $mSiO_2$ in the superparticles but without the polymeric nanofibers. The nitrogen sorption isotherm of the control $mSiO_2$ for comparison was obtained, which has a similar shape to that of the superparticles, and a step at relative pressure of 0.26; the pore size of control $mSiO_2$ is about 2 nm. In literature, when $mSiO_2$ was prepared under the same conditions, the pore size is also about 2 nm (the isotherm has a step at relative pressure of 0.26), as reported Zhao et al (D. Y. Zhao et al., J. Am. Chem. Soc. 2007, 130, 28-29). It is known that $mSiO_2$ with a larger pore size has a step at higher relative pressure in nitrogen sorption isotherm (G. D. Stucky et al., Chem. Mater.

1996, 8, 1147-1160). We also noted that the isotherm of $mSiO_2$ has a step at relative pressure of approximately 0.4 (corresponding to the pore size of 3 nm) has been reported (G. D. Stucky et al., Science 268, 1324 (1995)). The difference in the pore sizes results from the difference in the conditions for preparing the $mSiO_2$.

S5. The dissociation of superparticles supports the conclusion that the hybrid nanofibers are coated by PEG chains

The suspending particles formed at 34 min can dissociate into hybrid nanofibers by adding excess HCl into the suspension. The dissociation indicates that there is no covalent linkage between the hybrid nanofibers within the superparticles. It should be attributed to the existence of PEG chains coated on the surface of the hybrid nanofibers; without the protection of the PEG chains on the surface of the hybrid nanofibers, they should have been cross-linked during the hydrolysis of TEOS.

S6. Explanation of self-limited aggregation

Actually, although there are examples reporting self-limited aggregation of particles in literature, we cannot find its distinct definition in these examples. Usually, when the aggregation in a system stops automatically while the factors driving the aggregation remain unchanged, and the aggregates are dispersible in the suspension, the aggregation can be named as self-limited aggregation. In the present study, the aggregation was driven by the reaction of TEOS and the resultant deposition of $mSiO_2$ onto the nanofibers. As indicated in Figure 4A in the main text, the reaction and the deposition lasted for more than 2 hours. However, the aggregation stopped automatically 40 minutes after beginning of the reaction and deposition and the resultant superparticles were dispersible in the suspension; this aggregation has all the abovementioned features for the self-limited aggregation. Therefore, we named the aggregation of the hybrid nanofibers as self-limited aggregation.

S7. The micrometer-sized superparticles can be separated easily by centrifugation or filtration

The superparticles sized 35 μm on average, and thus can be separated easily by centrifugation. To determine the residue concentration of the superparticles after centrifugation, the superparticles were agitated with deionized water, and the supernatant after centrifugation was collected and freeze-dried. The weight of superparticles from 500 mL supernatant was 4 mg, i.e., the residue concentration of the superparticles in the supernatant is as low as 8 μg/mL. Filtration can also be used to remove the superparticles. The filtered solution has a weaker light scattering intensity than that of the supernatant after centrifugation, which indicates that the amount of residue superparticles by filtration is lower.

S8. Determination of the degree of labeling of the BSA-RhB conjugates

The degree of labeling is the number of dye molecules per protein molecule, which can be calculated from the UV-vis spectrum by using the Beer-Lambert law. The concentration of the dye can be determined by the absorption at visible regions. And

by subtraction of the absorption of the dye at 278 nm, the concentration of BSA can also be determined.

S9. About the repeated use of the superparticles

We tried to remove the adsorbed rhodamine B from the used superparticles. We washed the used superparticles by excess water, excess ethanol and extensive extraction by hot acetone successively, but, although a considerable part of the adsorbed rhodamine B was removed, the superparticles after the treatment still carry a portion of rhodamine B on them as indicated by the red color of rhodamine B on the superparticles (see the photographs below that are taken at each stage of the treatment). So we don't recommend the repeated use of the superparticles.

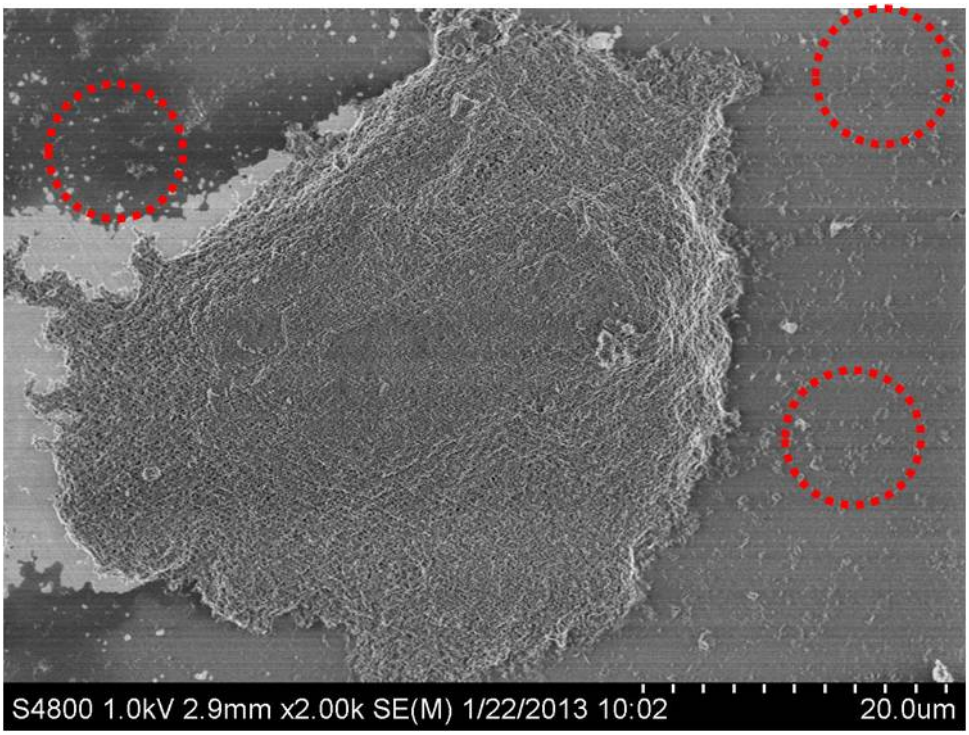

Figure S1. SEM image of the suspending particles formed at reaction time of 34 min and the coexisting small clusters of hybrid nanofibers (indicated by the red dashed circles).

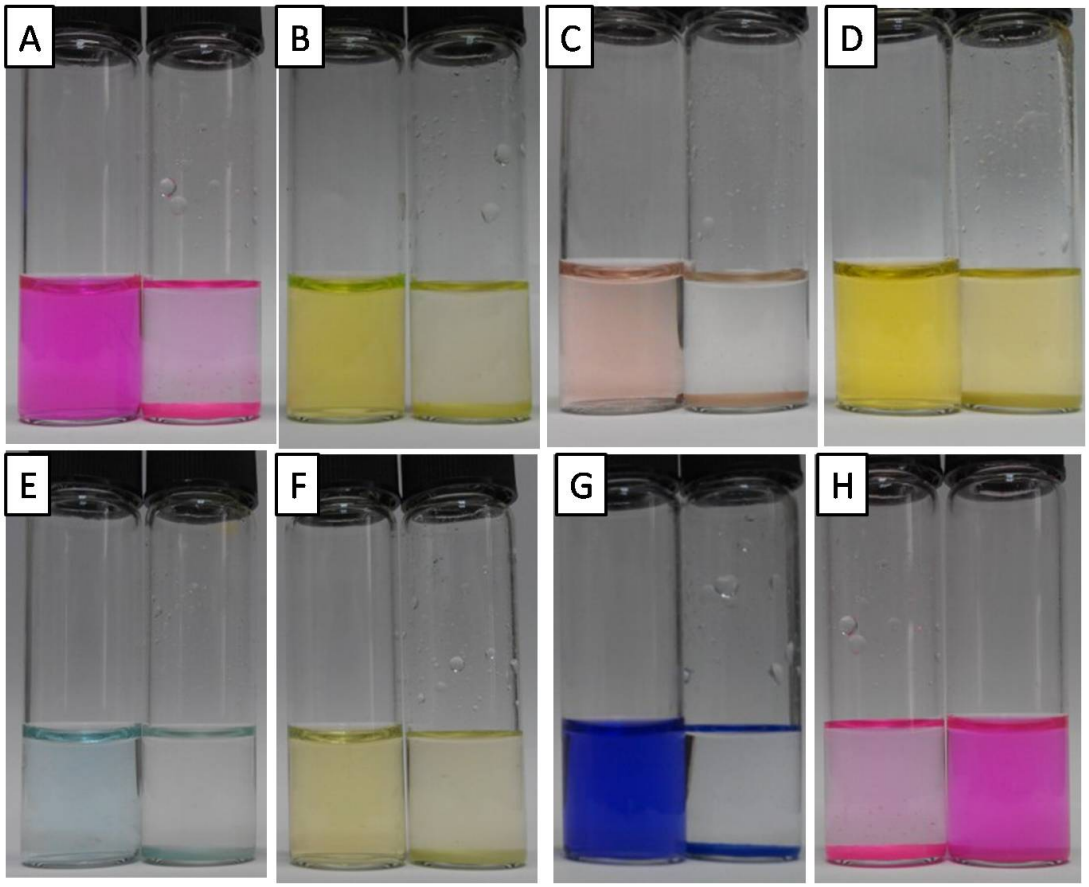

Figure S2. (A-G) Test of the adsorption capability of the meso/macro bimodal porous superparticles by various organic dyes (30 μg dye in 3.6 mL 0.2 M $NaHCO_3$ buffer (pH=9), 12 mg superparticles). A, rhodamine B; B, fluorescein isothiocyanate; C, congo red; D, methyl red; E, light green; F, basic yellow; G, basic violet. In A-G, the bottle on the right is the sample after dye absorption by superparticles and the bottle on the left is for control (without addition of superparticles). (H) Adsorption of rhodamine B by mesoporous superparticles (left) and amorphous superparticles (right). The preparation of amorphous superparticles was similar to that of mesoporous superparticles, but without the addition of CTAB. The result indicates that the adsorption of rhodamine B can be attributed to the silica mesopores on the superparticles.

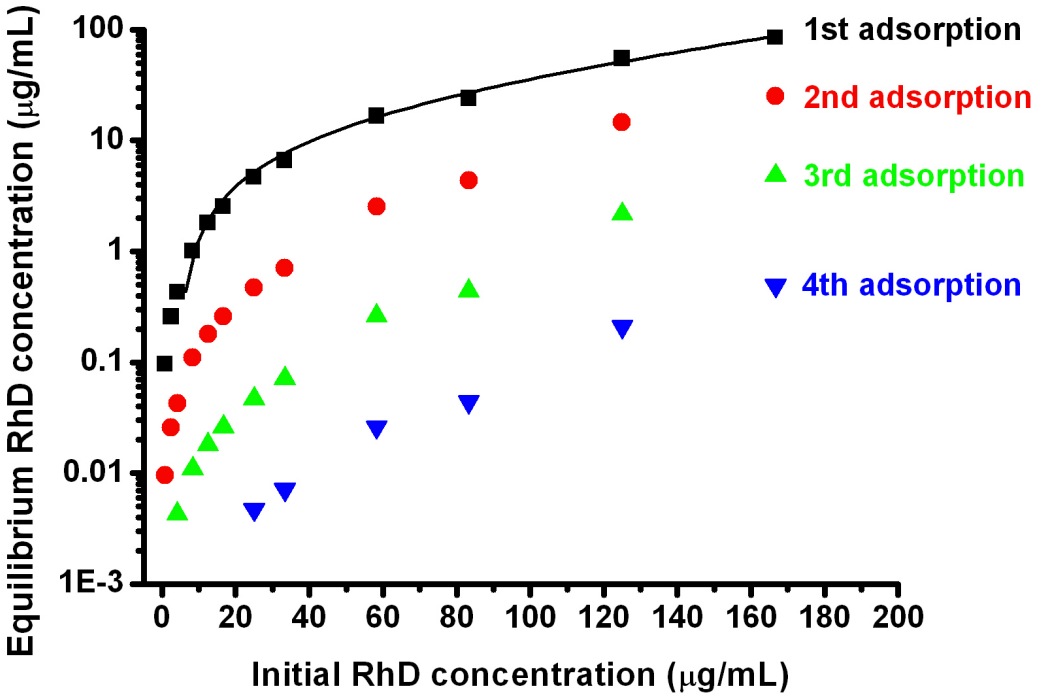

Figure S3. Plot of equilibrium RhB concentration after each adsorption against initial RhB concentration. For 1st adsorption, 4 mg superparticles were mixed with 1.2 mL RhB solution in 0.2 M $NaHCO_3$ for 1 h, and then removed by centrifugation. The RhB concentration in the supernatant was determined by UV-vis instrument. The curve of 1st adsorption is the curve of adsorption thermodynamic of RhB by the superparticles. Based on the curve of 1st adsorption, we calculated the equilibrium RhB concentration after 2nd ,3rd ,4th adsorption. For RhB solution with concentration lower than 0.1 μg/mL, it is hard for us to determine the equilibrium RhB concentration by using UV-vis spectrometer. Considering that the adsorption rate of RhB solution at low concentrations can reach 90%, we assume that, after adsorption of RhB solution with concentration lower than 0.1 μg/mL, the equilibrium concentration have a 10 fold reduction.